

# Structural stability and Raman scattering of InN nanowires under high pressure

L.D. Yao, S.D. Luo, X. Shen, S.J. You, L.X. Yang, and S.J. Zhang  
*Beijing National Laboratory for Condensed Matter Physics, Institute of Physics,  
Chinese Academy of Sciences, Beijing 100190, People's Republic of China*

S. Jiang, Y.C. Li, and J. Liu  
*Institute of High Energy Physics, Chinese Academy of Sciences,  
Beijing 100039, People's Republic of China*

K. Zhu, Y.L. Liu, W.Y. Zhou, L.C. Chen, C.Q. Jin, R.C. Yu,<sup>a)</sup> and S.S. Xie  
*Beijing National Laboratory for Condensed Matter Physics, Institute of Physics,  
Chinese Academy of Sciences, Beijing 100190, People's Republic of China*

(Received 3 November 2009; accepted 18 June 2010)

High-pressure in situ angular dispersive x-ray diffraction study on the wurtzite-type InN nanowires has been carried out by means of the image-plate technique and diamond-anvil cell (DAC) up to about 31.8 GPa. The pressure-induced structural transition from the wurtzite to a rocksalt-type phase occurs at about 14.6 GPa, which is slightly higher than the transition pressure of InN bulk materials ( $\sim 12.1$  GPa). The relative volume reduction at the transition point is close to 17.88%, and the bulk modulus  $B_0$  is determined through fitting the relative volume-pressure experimental data related to the wurtzite and rocksalt phases to the Birch–Murnaghan equation of states. Moreover, high-pressure Raman scattering for InN nanowires were also investigated in DAC at room temperature. The corresponding structural transition was confirmed by assignment of phonon modes. We calculated the mode Grüneisen parameters for the wurtzite and rocksalt phases of InN nanowires.

## I. INTRODUCTION

In the past several years, the functional semiconductors, such as GaN, AlN, ZnS, and ZnSe, have become the focus materials in the research for the fabrication of photoelectronic devices.<sup>1–6</sup> In the case of III–V nitrides, their large direct band gap makes them suitable for photoelectronic applications in the blue and ultraviolet spectral regions. Many publications<sup>7–9</sup> have been concentrated on characterizing as accurately as possible their important optical and electrical properties. Furthermore, several groups<sup>10–14</sup> also paid attention to their structures and physical properties under different conditions. However, as an important member of the III–V nitrides, InN was the least studied because of the difficulty in growing high quality material. Recently, with the progress in growth techniques, high quality InN has been prepared successfully. Among all the III-nitride compounds, it was believed that InN has the lowest effective electron mass,<sup>15</sup> potentially leading to a semiconductor with high mobility. Moreover, while the band structures of GaN and AlN are relatively well understood, the band

parameters of InN are still under debate. Recent measurement results suggested that InN has an unexpectedly low band gap of 0.7–0.9 eV<sup>16</sup> rather than 1.8–2.1 eV as previously reported.<sup>15</sup> Various experiments, such as a recent Mie resonances study by Shubina et al.,<sup>17</sup> have been carried out to explain the discrepancy. Nevertheless, the growth of thick undoped InN layers with high structural quality is still very difficult.<sup>18</sup> Thus far, the knowledge of InN properties remains still rather poor. Therefore, it is very necessary to thoroughly study this kind of material.

It is well known that the structural transition has a large effect on the physical properties. Certainly, it is also very important to understand the relationship between the structure and properties for these kinds of functional semiconductor materials. As a tunable thermodynamic parameter, the external pressure plays an important role in materials science. This pressure can affect not only the crystal structure, but also the electronic structure. In the case of InN, Ueno et al.<sup>10</sup> already studied its structural stability and pointed out that InN undergoes a phase transition from the wurtzite-type to a rocksalt-type structure at 12.5 GPa. Later, some groups<sup>11,12</sup> also confirmed the structural transition by means of Raman scattering experiments under

<sup>a)</sup>Address all correspondence to this author.

e-mail: rcyu@aphy.iphy.ac.cn

DOI: 10.1557/JMR.2010.0290

hydrostatic pressure, and analyzed the behavior of the  $E_2$  and longitudinal optical  $A_1(\text{LO})$  phonons of hexagonal InN phase at different pressures. The aforementioned study mainly focused on InN powders or thin films, rather than a low dimensional one. In this work, we report on the study of the structural stability of one-dimensional (1D) InN nanowires using the high-pressure in situ angular dispersive x-ray diffraction (ADXRD) technique. In addition, linear pressure coefficients and mode Grüneisen parameters of InN phonons are determined by the Raman spectroscopy analysis.

## II. EXPERIMENTAL DETAILS

The 1D InN nanowires were synthesized by nitriding  $\text{In}_2\text{O}_3$  powders in an ammonia flux in a tubular furnace described previously.<sup>19,20</sup> The detailed process is described in Ref. 21. The average diameter of the InN nanowires is about 100 nm.

Angle-dispersive powder x-ray diffraction experiments on InN nanowires up to 31.8 GPa at room temperature were performed at 4W2 beamline of Beijing Synchrotron Radiation Facility (BSRF, IHEP, Beijing). The x-ray wavelength was 0.06165 nm and beam size was 25  $\mu\text{m}$  in diameter. The diffracted x-ray was detected with an imaging plate. High pressure was generated using a symmetric-type diamond-anvil cell (DAC) with 400- $\mu\text{m}$  culets. The silicon oil was used as pressure transmitting medium to obtain a hydrostatic pressure condition. Pressures were calibrated by the ruby luminescence technique.

For the Raman scattering experiments, the InN nanowires were carefully loaded into a 250- $\mu\text{m}$  stainless steel gasket hole, and then installed into a symmetric-type DAC with 400- $\mu\text{m}$  culets. Here, a mixture of 4:1 methanol-ethanol was used as a pressure transmitting medium for the sake of the better hydrostatic conditions. Pressures were also calibrated by the ruby luminescence technique. Raman spectra were recorded in backscattering geometry in the frequency region from 100 to 1000  $\text{cm}^{-1}$ , using a LABRAM-HR confocal laser Micro-Raman spectrometer (HR800, HORIBA Jobin Yvon, Paris, France). The 532-nm line of the Verdi-2 solid-state laser was used as a Raman excitation source. A 25 $\times$  microscope objective lens was applied to focus the laser beam and collect the scattered light. The instrument resolution was 1  $\text{cm}^{-1}$ . All the measurements were carried out at room temperature.

## III. RESULTS AND DISCUSSION

### A. High-pressure in situ ADXD

The InN bulk material crystallizes in the wurtzite-type structure with a space group of  $P6_3mc$  at ambient conditions. For InN nanowires, it possesses the same structure as the InN bulk material. Figure 1 shows the

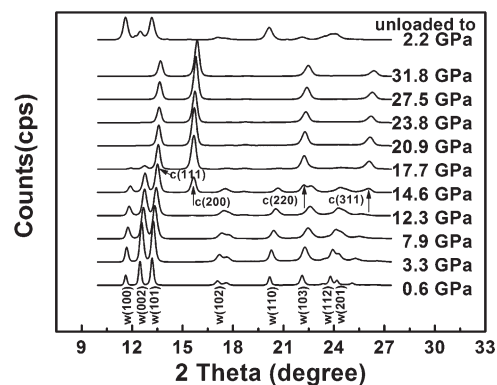


FIG. 1. High-pressure in situ ADXD patterns of InN nanowires.

high-pressure in situ ADXD patterns of InN nanowires up to about 31.8 GPa. It can be seen that all the diffraction peaks shift to the right side with increasing pressure due to the reduction of unit cell volume. Upon the application of pressure, the wurtzite phase persists up to around 14.6 GPa. Above this pressure, all the peaks of the wurtzite-type phase become very weak and a few new peaks appear, indicating that a phase transition takes place. Beyond about 20.9 GPa, all the peaks of the wurtzite-type phase disappear and instead four new peaks appear. According to the relevant report,<sup>10</sup> these new peaks can be assigned to (111), (200), (220), and (311) reflections of a rocksalt-type structure. Therefore, the transition in InN nanowires is viewed as being from the wurtzite to a rocksalt structure. However, it should be noted that the transition pressure ( $\sim 14.6$  GPa) for the InN nanowires is slightly higher than for InN bulk materials (12.1 GPa). Generally, nanometer materials like nanowires have considerable surface and thus store much higher surface energy than bulk materials. Hence, it is easy to understand that InN nanowires need a higher pressure than InN bulk materials to overcome the extra surface energy to realize the phase transition. The top of Fig. 1 displays the diffraction pattern collected after releasing the pressure from maximum pressure in our experiments. Obviously, the diffraction peaks of the wurtzite phase reappear and merely possess different intensities resulting from the variation of the orientation of grains [may change to (100)], suggesting that InN nanowires have a reversible phase transition.

In addition, the lattice parameters  $a$  and  $c$  for the wurtzite phase of InN nanowires are plotted in Fig. 2(a) as a function of pressure. Obviously, both the lattice parameters  $a$  and  $c$  show a monotonic decrease with increasing pressure, but the  $c$ -axis length seems to go down faster around 14.6 GPa as compared to  $a$ -axis length, which is similar to the behavior in bulk material InN. The axis ratio  $c/a$  is also displayed in Fig. 2(b). At ambient pressure, the ratio is about 1.613 close to the reported value in bulk materials,<sup>10</sup> however, a rapid fall

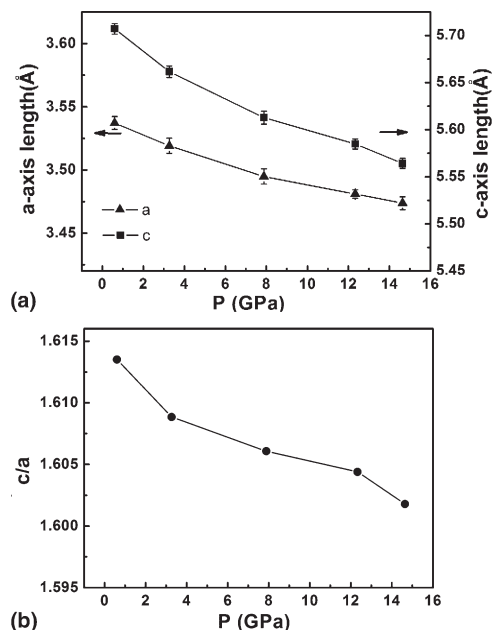


FIG. 2. (a) Axis lengths and (b)  $c/a$  ratio of the wurtzite phase as a function of pressure.

around 14.6 GPa is clearly visible as a result of the variation of  $a$ - and  $c$ -axis lengths. In Fig. 3, the lattice parameter  $a$  for the rocksalt phase exhibits a reducing trend as the pressure rises. We also studied the relative volume change of the InN nanowires as a function of pressure, as shown in Fig. 4. For the wurtzite phase, the relative volume exhibits a monotonous decrease with increasing pressure to 14.6 GPa. However, there is a drastic reduction in the relative volume at 14.6 GPa accompanied by the phase transition from the wurtzite to the rocksalt structure, and the relative volume reduction at the transition point is close to 17.88%. The bulk modulus  $B_0$  is obtained through fitting the relative volume-pressure experimental data related to the wurtzite and rocksalt phases to the Birch–Murnaghan equation of states. The obtained  $B_0$  are 131.0 GPa ( $B_0' = 12.7$ ) and 205.1 GPa ( $B_0' = 5.0$ ) for the former and latter, respectively, which are higher than that of InN bulk materials (125.5 GPa for the wurtzite phase,  $B_0' = 12.7^{10}$ ; 170.0 GPa for the rocksalt phase,  $B_0' = 5.0^{22}$ ). This indicates that it is difficult to compress the InN nanowires due to size effect.

## B. Raman scattering of InN nanowires under high pressures

Raman scattering has proved to be a powerful tool for studying physical properties such as determination of phonon modes. In the case of InN, group theory analysis predicted that there are six phonon modes (irreducible representation:  $\Gamma = A_1 + 2B_1 + E_1 + 2E_2$ ) for the compound with  $P6_3mc$ , where the polar phonon modes

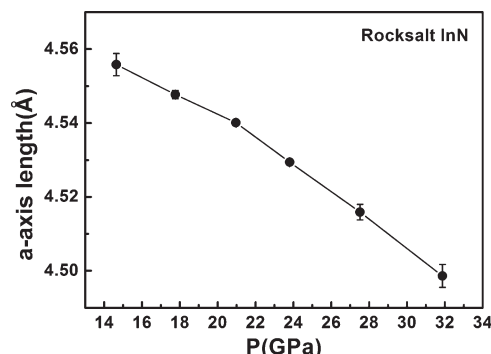


FIG. 3. Variations of axis length of the rocksalt phase with increasing pressure.

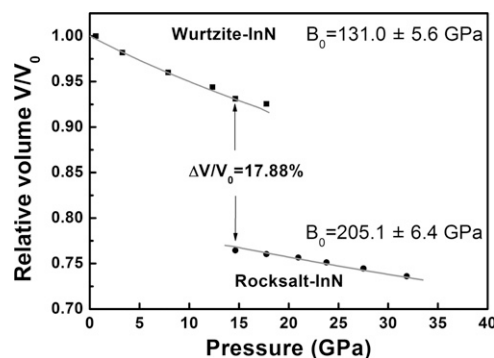


FIG. 4. Relative volume of InN nanowires as a function of pressure.

of  $A_1$  and  $E_1$  symmetries are both Raman and infrared active, whereas the nonpolar  $E_2$  modes are Raman active only, and the  $B_1$  modes are silent.<sup>23</sup> Therefore, the wurtzite InN possesses four Raman active phonon modes. In our experiments, the Raman scattering spectra of InN nanowires were studied at different pressures. To monitor the possible influence of Raman scattering signals from transmitting pressure medium, we successively collected two sets of Raman spectra from the sample area and neighboring transmitting medium region at each pressure point, respectively. Due to the negligible scattering signals from the transmitting medium, it is believed that no remarkable influence takes place on the Raman scattering peaks of InN nanowires. Therefore, the Raman spectra of InN nanowires are available by subtracting background. In Fig. 5, the Raman spectra after subtracting background with increasing pressure up to 32.9 GPa are displayed in the frequency range from 300 to 1000  $\text{cm}^{-1}$ . Clearly, one can see the broadening of the Raman peaks probably resulting from structural disordering of the InN nanowires. The three main peaks, observed at around 440, 503, and 590  $\text{cm}^{-1}$  in Raman spectra at about 2.5 GPa, can be assigned to transverse optical  $A_1(\text{TO})$ ,  $E_2(\text{high})$ , and  $A_1(\text{LO})$ , respectively, in agreement with the Raman selection rules for the wurtzite structure. With the increase of pressure, Raman peaks gradually shift to high frequency. When

the pressure is at about 14.5 GPa, a new Raman peak located at  $580\text{ cm}^{-1}$  [marked by (a)] appears on the left side of  $A_1(\text{LO})$  mode, indicating that the crystal structure of the InN nanowires begins to change beyond this pressure. At 15.3 GPa, the phonon modes of the wurtzite phase are basically vanishing and the other two new peaks are observed at  $417$  and  $623\text{ cm}^{-1}$  [marked by (b) and (c), respectively]. Compared with the above results of ADXD, these new peaks may be associated with a structural transition from the wurtzite to the rocksalt at the nearly corresponding pressure. Above 15.3 GPa, the phonons of the wurtzite structure are invisible, while all the new phonon modes shift to higher frequency with increasing pressure up to 32.9 GPa. As the pressure is gradually released to about 1.6 GPa, the new Raman peaks vanish while the original peaks related to the wurtzite phase reappear, further attesting the reversible transition between the wurtzite and rocksalt phases of the InN nanowires.

In fact, according to the corresponding reports, the first-order Raman scattering is theoretically forbidden in the light of the selection rules for the case of the rocksalt structure, therefore Raman peaks should disappear beyond the phase transition pressure. However, a few abnormal peaks [marked as (a), (b), and (c)] are visible in our experiments. Similarly, Pinquier et al.<sup>12</sup> also observed the strong Raman scattering signal beyond the

phase transition in the InN flakes. For the abnormal case, some research results of GaN can be considered for explanation. Generally, a structural transition to the rocksalt-type takes place in GaN at about 52.2 GPa.<sup>10</sup> By comparing experimental Raman spectra acquired under high pressure with ab initio calculations in the case of GaN, Halsall et al.<sup>24</sup> pointed out that the Raman signal assigned to the rocksalt (cubic) structure was associated to disorder activated scattering by the phonon density of state (DOS). Therefore, it is assumed that Raman scattering behavior of nanowire InN under high pressure may be similar to that of GaN. In the case of InN nanowires, it is possible that the phase transition in the nano-scale area simultaneously takes place everywhere, resulting in a high degree of disorder as the origin of the phonon DOS scattering.<sup>10</sup> However, so far the DOS calculations for the InN rocksalt-phase have only been investigated for zero pressure,<sup>25</sup> whereas the relevant studies for the case of high pressure are desired to be carried out. Therefore, we prefer to assign the vibrational modes observed in the rocksalt structure to the DOS scattering.

The pressure dependences of Raman phonon frequencies in the compression process from 2.5 to 32.9 GPa are shown in Fig. 6. Generally speaking, the frequency versus pressure can be expressed by a quadratic relationship for most semiconductors. Considering that the second order term is negligible in our experiments, the frequency of phonon can be fitted approximately using only a linear equation  $\omega_i = \omega_{i0} + K_i^H p$ ,<sup>11</sup> where  $\omega_{i0}$  is the frequency of the  $i$ th phonon at zero pressure, and  $K_i^H = (\partial\omega_i/\partial p)_{p=0}$  is the linear pressure coefficient. In Fig. 6, the fittings are illustrated by the solid lines for the observed phonons of the wurtzite and rocksalt structures, respectively. The  $K_i^H$  values can be gained by the slopes of phonon frequency versus pressure curves, as well as the zero pressure frequencies are regressed by the fittings, and the corresponding values are listed in Table I. These results are available to calculate the mode Grüneisen parameters, which can be determined from the pressure coefficients using the formula

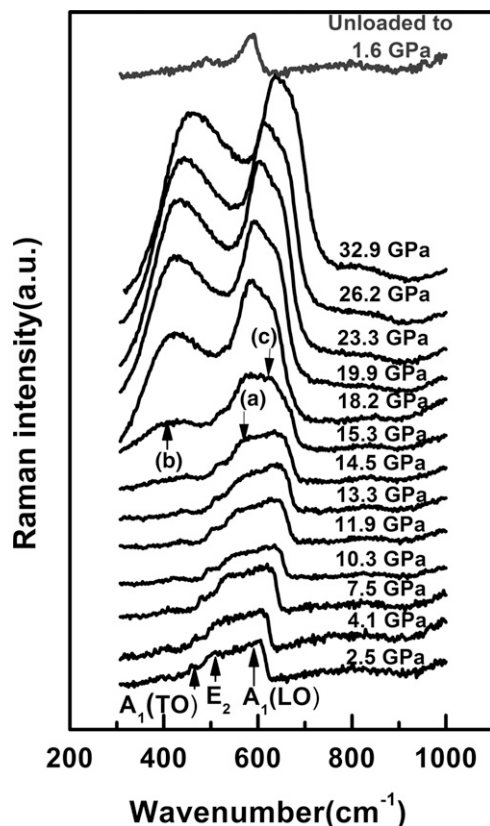


FIG. 5. High-pressure Raman scattering spectra of InN nanowires.

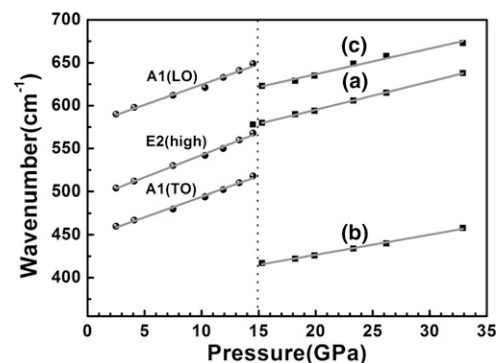


FIG. 6. The phonon wave numbers of InN nanowires versus pressure. Left part: the wurtzite structure; Right part: the rocksalt structure.



TABLE I. Results of linear regressions  $\omega_{i0}$  and  $K_i^H$  and calculated mode Grüneisen parameters  $\gamma_i$  using the values of the bulk modulus obtained from the high-pressure ADXD experiments.

InN nanowires	Phonon modes $i$	$\omega_{i0}$ ( $\text{cm}^{-1}$ )	$K_i^H$ ( $\text{cm}^{-1} \text{GPa}^{-1}$ )	$\gamma_i$
Wurtzite	$A_1(\text{TO})$	446	5.10	1.49
	$E_2(\text{high})$	490	4.74	1.26
	$A_1(\text{LO})$	577	4.73	1.07
Rocksalt	(b)	379	2.34	1.26
	(a)	529	3.20	1.24
	(c)	576	2.90	1.03

$\gamma_i = -\partial \ln \omega_i / \partial \ln V = B_0 / \omega_{i0} K_i^H$ .<sup>26,27</sup> In the above ADXD experiments, it is known that the obtained bulk moduli  $B_0$  are 131.0 GPa ( $B_0' = 12.7$ ) and 205.1 GPa ( $B_0' = 5$ ) for the wurtzite and rocksalt phases, respectively. Thus, the corresponding mode Grüneisen parameters are calculated and given in Table I as well. The values for the different modes are close to results reported by Pinquier et al.,<sup>12</sup> however, the slight discrepancy can be explained by the larger bulk modulus values for the InN nanowires.

#### IV. CONCLUSIONS

The high-pressure in situ ADXD and Raman experiments were performed for the wurtzite-type InN nanowires at ambient temperature. Both experiments indicate that the InN nanowires undergo a structural transition from the wurtzite to the rocksalt-type at about 14.6 GPa, which is slightly higher than the transition pressure of InN bulk materials (12.1 GPa). Moreover, there is a drastic reduction of about 17.88% in the relative volume at 14.6 GPa accompanied by the phase transition. By fitting the relative volume versus pressure, bulk moduli  $B_0$  are determined as 131.0 GPa ( $B_0' = 12.7$ ) and 205.1 GPa ( $B_0' = 5$ ) for the wurtzite and the rocksalt phase, which are slightly higher than that of InN bulk materials (125.5 GPa for the wurtzite phase,  $B_0' = 12.7^{10}$ ; 170.0 GPa for the rocksalt phase,  $B_0' = 5.0^{22}$ ). The observed abnormal Raman signals in the rocksalt-type (cubic) phase are considered to be associated with the scattering of phonon DOS. The corresponding mode Grüneisen parameters are obtained from the experimental data. In contrast to the previous reports, the slight discrepancy for the mode Grüneisen parameters can be explained by the larger bulk modulus values for the InN nanowires. In a word, InN nanowires show a reversible phase transition in either high-pressure ADXD or Raman scattering experiments.

#### ACKNOWLEDGMENTS

This work was supported by the National Natural Science Foundation of China (Grant No. 50921091), the State Key Development Program for Basic Research of China (Grant No. 2005CB623602), and Specific funding

of Discipline and Graduate Education Project of Beijing Municipal Commission of Education.

#### REFERENCES

1. S. Nakamura: III-V nitride based light-emitting devices. *Solid State Commun.* **102**, 237 (1997).
2. J.W. Orton and C.T. Foxon: Group III nitride semiconductors for short wavelength light-emitting devices. *Rep. Prog. Phys.* **61**, 1 (1998).
3. S.C. Jain, M. Willander, J. Narayan, and R.V. Overstraeten: III-nitrides: Growth, characterization, and properties. *J. Appl. Phys.* **87**, 965 (2000).
4. M.A. Haase, J. Qiu, J.M. Depuydt, and H. Cheng: Blue-green laser diodes. *Appl. Phys. Lett.* **59**, 1272 (1991).
5. H. Jeon, J. Ding, A.V. Nurmikko, W. Xie, D.C. Grillo, M. Kobayashi, and R.L. Gunshor: Blue-green injection laser diodes in (Zn,Cd)Se/ZnSe quantum wells. *Appl. Phys. Lett.* **59**, 3619 (1991).
6. J. Gaines, R. Drenten, K.W. Haberen, T. Marshall, P.M. Mensz, and J. Petruzzello: Blue-green injection lasers containing pseudomorphic  $\text{Zn}_{1-x}\text{Mg}_x\text{S}_y\text{Se}_{1-y}$  cladding layers and operating up to 394 K. *Appl. Phys. Lett.* **62**, 2462 (1993).
7. S.K. O'Leary, B.E. Foutz, M.S. Shur, U.V. Bhapkar, and L.F. Eastman: Electron transport in wurtzite indium nitride. *J. Appl. Phys.* **83**, 826 (1998).
8. B.E. Foutz, S.K. O'Leary, M.S. Shur, and L.F. Eastman: Transient electron transport in wurtzite GaN, InN, and AlN. *J. Appl. Phys.* **85**, 7727 (1999).
9. J. Chen, G. Cheng, E. Stern, M.A. Reed, and Ph. Avouris: Electrically-excited infrared emission from InN transistors. *Nano Lett.* **7**, 2276 (2007).
10. M. Ueno, M. Yoshida, A. Onodera, O. Shimomura, and K. Takemura: Stability of the wurtzite-type structure under high pressure: GaN and InN. *Phys. Rev. B* **49**, 14 (1994).
11. C. Pinquier, F. Demangeot, J. Frandon, J.W. Pomeroy, M. Kuball, H. Hubel, N.W.A. van Uden, D.J. Dunstan, O. Briot, B. Maleyre, S. Ruffenach, and B. Gil: Raman scattering in hexagonal InN under high pressure. *Phys. Rev. B* **70**, 113202 (2004).
12. C. Pinquier, F. Demangeot, J. Frandon, J.-C. Chervin, A. Polian, B. Couzinet, P. Munsch, O. Briot, S. Ruffenach, B. Gil, and B. Maleyre: Raman scattering study of wurtzite and rocksalt InN under high pressure. *Phys. Rev. B* **73**, 115211 (2006).
13. V.Yu. Davydov, V.V. Emtsev, I.N. Goncharuk, A.N. Smirnov, V.D. Petrikov, V.V. Mamutin, V.A. Vekshin, S.V. Ivanov, M.B. Smirnov, and T. Inushima: Experimental and theoretical studies of phonons in hexagonal InN. *Appl. Phys. Lett.* **75**, 3297 (1999).
14. K. Sarasamak, A.J. Kulkarni, M. Zhou, and S. Limpijumnong: Stability of wurtzite, unbuckled wurtzite, and rocksalt phases of SiC, GaN, InN, ZnO, and CdSe under loading of different triaxialities. *Phys. Rev. B* **77**, 024104 (2008).
15. A. Bhuiyan, A. Hashimoto, and A. Yamamoto: Indium nitride (InN): A review on growth, characterization, and properties. *J. Appl. Phys.* **94**, 2779 (2003).
16. J. Wu, W. Walukiewicz, K.M. Yu, W.J. Auger III, E.E. Haller, H. Lu, W.J. Schaff, Y. Saito, and Y. Nanishi: Unusual properties of the fundamental band gap of InN. *Appl. Phys. Lett.* **80**, 3967 (2002).
17. T.V. Shubina, S.V. Ivanov, V.N. Jmerik, D.D. Solnyshkov, V.A. Vekshin, P.S. Kop'ev, A. Vasson, J. Leymarie, A. Kavokin, H. Amano, K. Shimono, A. Kasic, and B. Monemar: Mie resonances, infrared emission, and the band gap of InN. *Phys. Rev. Lett.* **92**, 117407 (2004).
18. Y. Nanishi, Y. Saito, and T. Yamaguchi: RF-molecular-beam-epitaxy growth and properties of InN and related alloys. *Jpn. J. Appl. Phys.* **42**, 2549 (2003).

19. S.D. Luo, W.Y. Zhou, Z.X. Zhang, L.F. Liu, X.Y. Dou, J.X. Wang, X.W. Zhao, D.F. Liu, Y. Gao, L. Song, Y.J. Xiang, J.J. Zhou, and S.S. Xie: Synthesis of long indium nitride nanowires with uniform diameters in large quantities. *Small* **1**, 1004 (2005).
20. S.D. Luo, W.Y. Zhou, Z.X. Zhang, X.Y. Dou, L.F. Liu, X.W. Zhao, D.F. Liu, L. Song, Y.J. Xiang, J.J. Zhou, and S.S. Xie: Bulk-quantity synthesis of single-crystalline indium nitride nanobelts. *Chem. Phys. Lett.* **411**, 361 (2005).
21. S.D. Luo, L.D. Yao, W.G. Chu, J. Shen, Z.X. Zhang, J.B. Li, J.H. Yi, R.C. Yu, W.Y. Zhou, and S.S. Xie: InN/In<sub>2</sub>O<sub>3</sub> peapod nanostructures and conformal conversion templated from InN counterparts via thermal oxidation. *Nanotechnology* **18**, 235605 (2007).
22. S. Uehara, T. Masamoto, A. Onodera, M. Ueno, O. Shimomura, and K. Takemura: Equation of state of the rocksalt phase of III–V nitrides to 72 GPa or higher. *J. Phys. Chem. Solids* **58**, 2093 (1997).
23. C.A. Arguello, D.L. Rousseau, and S.P.S. Porto: First-order Raman effect in wurtzite-type crystals. *Phys. Rev.* **181**, 1351 (1969).
24. M.P. Halsall, P. Harmer, P.J. Parbrook, and S.J. Henley: Raman scattering and absorption study of the high-pressure wurtzite to rocksalt phase transition of GaN. *Phys. Rev. B* **69**, 235207 (2004).
25. G. Kaczmarczyk, A. Kaschner, S. Reich, A. Hoffmann, C. Thomsen, D.J. As, A.P. Lima, D. Schikora, K. Lischka, R. Averbeck, and H. Riechert: Lattice dynamics of hexagonal and cubic InN: Raman-scattering experiments and calculations. *Appl. Phys. Lett.* **76**, 2122 (2000).
26. M. Blackman: On the thermal expansion of solids. *Proc. Phys. Soc. London, Sect. B* **70**, 827 (1957).
27. W.B. Daniels: *Lattice Dynamics*, edited by R.F. Wallis (Pergamon Press, Oxford, 1965), p. 273.